JOURNAL OF CATALYSIS **179,** 350–360 (1998)
ARTICLE NO. CA982230

Characteristics of Mordenite-Type Zeolite Catalysts Deactivated by SO_2 for the Reduction of NO with Hydrocarbons

Moon Hyeon Kim, In-Sik Nam,[1] and Young Gul Kim

Research Center for Catalytic Technology, Department of Chemical Engineering, School of Environmental Engineering, Pohang University of Science & Technology (POSTECH)/Research Institute of Industrial Science & Technology (RIST), P.O. Box 125, Pohang 790-600, Korea

Received November 21, 1997; revised July 21, 1998; accepted July 23, 1998

The deactivation of mordenite-type zeolite catalysts for the selective reduction of NO by hydrocarbons in the presence of SO_2 was examined in a packed-bed flow reactor system. The physicochemical properties of the deactivated catalysts by SO_2 were extensively characterized by TGA, TPSR, XPS, Raman, XANES, the measurements of surface area and elemental analysis. Not only the surface area and sulfur content of the deactivated catalysts, but their TGA and TPSR patterns strongly suggest the formation of a sulfur species as a deactivating agent on the catalyst surface. It is also observed that the sulfur species exists in the form of sulfate (SO_4^{2-}) by XPS and Raman. It mainly causes the loss of NO removal activity of the catalysts. The sulfate species formed on the deactivated catalysts by SO_2 did not significantly alter the chemical environment of the copper ions contained in the zeolite catalysts such as CuHM and CuNZA. It does not exist in the form of cupric sulfate pentahydrate on the catalyst surface as revealed by Cu K-edge absorption spectra of the catalysts.

INTRODUCTION

Selective catalytic[1] reduction of NO_x by hydrocarbons has been investigated, not only as an alternative technology of NO_x reduction by NH_3 which is commercially available for the reduction of NO_x from stationary sources such as industrial and utility boilers but as a new technology reducing NO_x from the exhausts of lean-burn gasoline and diesel engines. A number of catalysts have been extensively examined by previous studies for this technology (1–10). Transition metal ion-exchanged zeolite catalysts, mainly MFI and MOR structure types such as ZSM-5 and mordenite exhibit a high catalytic performance among the catalysts developed so far.

Most of flue gas from the emission sources also contains H_2O vapor and SO_2, as well as NO_x, which may cause the loss of NO reducing activity of SCR catalysts. Therefore, their tolerances of the catalysts are essential for the successful commercial application of the catalytic process. Since the significant loss of NO removal activity of the transition metal ion-exchanged zeolite catalysts was observed for the reduction of NO by hydrocarbons in the wet feed stream (1, 4, 9, 11–13), the recent studies of this technology mainly concerned elucidation of the cause of the catalyst deactivation by H_2O (14–18). Therefore, the effect of SO_2 on the activity loss of the catalysts employing hydrocarbons as a reductant has not been widely studied yet.

The influence of SO_2 on the performance of Cu-ZSM-5 catalyst for NO reduction by C_3H_6 was reported by Iwamoto *et al.* (20), observing the slight decrease of the deNO_x activity by the addition of SO_2 to the feed gas stream during the course of reaction. The conversion of NO at the reaction temperature of 300°C, however, was completely recovered when the feed of SO_2 to the reaction stream was terminated. They suggested that the loss of the removal activity of the catalyst is probably due to the alteration of the copper ionic state on the catalyst surface. However, they did not further characterize the deactivated catalyst by SO_2 to elucidate the cause of the loss of NO removal activity.

A moderate deterioration of the deNO_x performance over Cu-mordenite catalyst for the reduction of NO by C_3H_8 with SO_2 was previously observed by Mabilon and Durand (21), while the performance of the oxidation reaction of C_3H_8 was significantly inhibited by SO_2. Although the recovery of the oxidation activity of C_3H_8 to CO_x was not observed by termination of the SO_2 feed to the reaction stream, NO conversion was immediately restored to the initial activity of NO removal. Recently, Li and Armor (22) also examined the effect of SO_2 with and without H_2O in the feed gas stream on the deNO_x efficiency of Co-ZSM-5 and Co-ferrierite catalysts for the reduction of NO by CH_4. Its effect on the catalytic performance for the reduction without H_2O strongly depends on the types of catalyst, as well as on the reaction temperatures. It is primarily due to the sulfur poisoning of cobalt ionic sites on the catalyst surface.

The study for the influence of SO_2 on the reduction of NO by hydrocarbons was not sufficiently made in the current literature to investigate the cause of the catalyst deactivation by SO_2. Furthermore, the deactivation mechanism of

[1] Corresponding author. E-mail: isnam@postech.ac.kr.

0021-9517/98 $25.00

zeolite catalysts for NO reduction by hydrocarbons with SO_2 was not well understood yet. The water tolerance of mordenite-type zeolite catalysts has been previously examined for the selective catalytic reduction of NO by hydrocarbons such as C_2H_4 and C_3H_6 (9, 16). Indeed, the cause of the catalyst deactivation by H_2O vapor included in the feed gas stream has been extensively studied for the same reaction system (16). When 1000 ppm of SO_2 was admitted to NO reduction by hydrocarbons over the zeolite catalysts, the sulfur tolerance of the catalyst has been also observed in the previous work (23).

In the present study, a deactivating agent formed on the surface of mordenite-type zeolite catalysts was identified to elucidate the cause of the loss of the deNO_x activity of the catalysts for NO removal reaction by SO_2. The role of Cu^{2+} ions on the catalyst surface attributed to the catalyst deactivation was also investigated by the characterization of the catalysts before and after reaction with TGA, TPSR, XPS, Raman, and XAS.

EXPERIMENTAL

Catalyst Deactivation by SO_2

Hydrogen mordenite (HM) and Cu-exchanged hydrogen mordenite (CuHM) were obtained from synthetic mordenite, Zeolon 900Na (PQ Corp.). A natural zeolite (NZ) mainly containing mordenite-type zeolite mined from Youngil, Korea was also employed to prepare CuNZA (copper ion-exchanged natural zeolite) catalyst (24). Following the procedure for ion exchanging, drying, and calcining as described in the previous studies (9, 16, 24), CuHM and CuNZA catalysts containing Cu ions of 3.5 (Cu/Al = 0.24) and 1.8 wt% (Cu/Al = 0.22), respectively, were employed in the present study.

The sulfur tolerance of mordenite-type zeolite catalysts such as HM, CuHM, and CuNZA for the selective reduction of NO by hydrocarbons has been observed in a fixed-bed flow reactor system with the reaction mixture, including 500 ppm of NO, 1000 ppm of C_2H_4 or 2000 ppm of C_3H_6, 4.2% of O_2, 1000 ppm of SO_2, and He as a balance gas (23). A detailed description of the reaction system and experimental conditions has been described in the previous works (9, 23). The deNO_x performance of the catalysts for NO removal reaction by hydrocarbons with SO_2 at the reaction temperatures of 360 and 400°C has been observed during more than 12 h of the reactor on-stream time, as also examined in the previous study (23).

Catalyst Characterization

Surface area and sulfur content measurements. The BET surface area of the deactivated catalysts by SO_2 was measured with a Micromeritics Accusorb 2100E using liquid N_2 at 77 K after the catalysts were pretreated *in vacuo* at 180°C for 10 h. The contents of sulfur and carbonaceous deposits on the surface of the deactivated catalysts were also determined by an oxidation method with a LECO SC-132 Sulfur Systems and CS-044 Carbon & Sulfur 781-000 Systems (LECO Co.).

Thermogravimetric analysis (TGA). The weight change of the deactivated catalysts by SO_2 was examined with a SEIKO I 300 instrument, using about 10 mg of sample and the heating rate of 10°C/min. TGA patterns were basically obtained within the temperature ranges from 25 to 800°C; 40 cm^3/min of the flow rate of high purity He (99.9999%) as a carrier gas was maintained during TGA analysis.

Temperature-programmed surface reaction (TPSR). TPSR for the catalysts deactivated by the reaction stream containing SO_2 has been examined with an on-line quadrupole mass spectrometer (MMPC-200D, VG Quadrupoles), which may provide the information on the composition of a deactivating agent and its adsorption strength on the catalyst surface. The deactivated catalyst was charged into a quartz U-shaped reactor with 1/4″OD. The reactor was surrounded by a cylindrical electric furnace which is readily controlled by a PID temperature controller with a K-type thermocouple. After the reactor is fully purged by He at 50°C, its temperature was ramped from 50 to 800°C at the ramping rate of 10°C/min for the identification of the desorbing compounds from the surface of the deactivated catalysts such as H_2O, CO, CO_2, CH_4, SO_2, and SO_3 by the mass spectrometer.

X-ray photoelectron spectroscopy (XPS). XPS spectra for the deactivated catalysts were observed by a Perkin-Elmer PHI 5400 XPS spectrometer using Mg Kα primary radiation (350 W). S and Cu 2p lines of the catalysts were mainly examined with their self-supporting wafer after the reduction of NO by hydrocarbons in the presence of SO_2. The pass energy of the instrument was set at 72 eV. An energy width of 200 meV was also chosen in the present study. A charging effect of the spectra was carefully corrected with a carbon peak at 284.6 eV as a standard.

Raman spectroscopy. Raman spectra for HM, CuHM, and CuNZA catalysts deactivated by SO_2 were observed by a Spex 20 spectrometer equipped with a Spex Datamate computer. The excitation of the zeolite catalysts has been made with 514.5 nm line of a Spectra Physics 171 Ar ion laser powered by a Spectra Physics 265 exciter. To minimize local heating effects, where the laser beam impinges on the catalyst surface, a rotating lens assembly was employed.

X-ray absorption spectroscopy (XAS). XAS experiments for copper containing catalysts such as CuHM and CuNZA were performed at Beam Line 7C of Photon Factory in National Laboratory for High Energy Physics (KEK-PF), Japan. The synchrotron radiation from the storage ring (2.5 GeV, 300–250 mA) was monochromatized

by a channel-cut Si (111) crystal monochromator. The samples were ground into powder and then pressed into self-supporting wafers without any binder. Cu K-edge absorption was examined for the Cu-exchanged catalysts at room temperature before and after reaction with SO_2, as well as for the reference chemicals such as $Cu(OH)_2$ and $CuSO_4 \cdot 5H_2O$.

RESULTS

Sulfur Tolerance of Mordenite-Type Zeolite Catalysts

As previously observed by Kim *et al.* (9), the $deNO_x$ performance of the synthetic and natural zeolite catalysts for NO removal reaction strongly depended on the types of hydrocarbon as a reductant. The synthetic mordenite catalysts such as HM and CuHM exhibited a significant NO reducing activity when C_2H_4 was employed as a reductant, while C_3H_6 was favorable for the reduction of NO over CuNZA catalyst. The influence of SO_2 on the $deNO_x$ activity of the catalysts has been examined for these two kinds of reaction condition (23) where the catalytic systems reveal the best $deNO_x$ performance.

Figure 1 shows the $deNO_x$ activity maintenance of the catalysts for NO removal reaction without and with SO_2. About 6.5×10^{-5} mmol/g·s of NO removal rate (NO conversion = 60%) over HM catalyst at 360°C was attained for NO reduction by C_2H_4 under the SO_2-free condition even during 11 h of the continuous operation of the reactor. However, its NO removal activity gradually decreased when 1000 ppm of SO_2 is introduced to the reaction system. After the initial loss less than 0.7×10^{-5} mmol/g·s of the removal rate (NO conversion = 10%) within 8 h, the catalytic activity is still in a decreasing mode. The $deNO_x$ performance of CuHM catalyst at the same reaction temperature decreased from the initial rate of reaction of 6.3×10^{-5} (NO conversion = 58%) to 4.0×10^{-5} mmol/g·s after 13 h of the reactor operation with SO_2. Although the activity maintenance of the catalyst containing copper ions without SO_2 is quite stable, the feed of SO_2 to the catalytic system caused more rapid loss of its NO removal activity than that of HM catalyst without Cu ions on the catalyst surface.

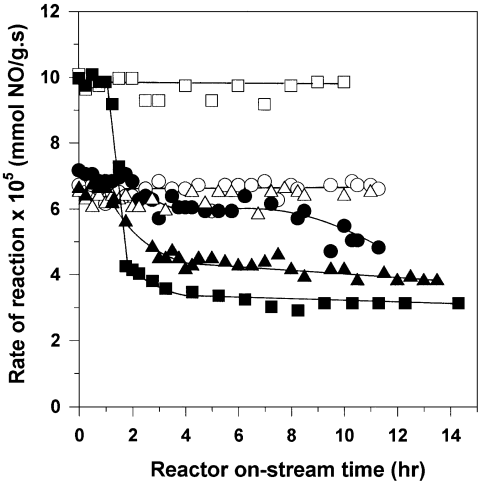

FIG. 1. Sulfur tolerance of HM (○, ●), CuHM (△, ▲) and CuNZA (□, ■) catalysts (○, △, □) without SO_2; (●, ▲, ■) with SO_2. Reaction condition: NO 500 ppm, C_2H_4 1000 (HM and CuHM) or C_3H_6 2000 ppm (CuNZA), O_2 4.2%, SO_2 1000 ppm, and $T = 360$°C (HM and CuHM) or 400°C (CuNZA).

TABLE 1

Physicochemical Properties of the Catalysts Deactivated by SO_2

Catalyst	Sulfur content (wt%)	BET surface area (m^2/g)	SO_4^{2-}/H^+ or Cu^{2+}
HM[a]	—	449	—
HM[b]	0.00	419	-
HM[c]	1.10	384	0.15
CuHM[a]	-	433	-
CuHM[b]	0.00	418	-
CuHM[c]	1.86	207	1.04
CuNZA[a]	-	210	-
CuNZA[b]	0.00	210	-
CuNZA[c]	0.54	139	0.59

[a] Fresh catalyst.
[b] After reaction without SO_2.
[c] After reaction with SO_2 of 1000 ppm.

In the absence of SO_2, the stable maintenance of the reaction rate of CuNZA catalyst for NO reduction by C_3H_6 at 400°C was also observed even for the reactor on-stream time of 10 h, as shown in Fig. 1. The decrease of the initial rate of NO removal reaction, however, was more than 60% when SO_2 is existing in the feed gas stream. No loss of NO removal activity due to carbonaceous compounds deposited on the catalysts was anticipated during the course of reaction without SO_2. The deteriorating trend for the oxidation reaction of the hydrocarbons such as C_2H_4 and C_3H_6 in the presence of SO_2 was also similar to that for NO removal reaction, regardless of the types of catalyst employed in the present study.

Characterization of Deactivated Catalysts by SO_2

BET surface area and sulfur content. The surface area of the mordenite-type zeolite catalysts even after the reduction of NO by hydrocarbons without SO_2 was quite similar to that of the fresh catalysts, as listed in Table 1 . It confirms that no carbonaceous compounds on the catalyst surface are attributed to the loss of the $deNO_x$ activity of the catalysts. About 10% loss of the surface area for HM catalyst was observed by SO_2, while more than 50% of the reduction of the area appeared for the deactivated CuHM catalyst. For CuNZA catalyst, about 30% of the surface area decreased by the feed of SO_2 to the reaction stream.

The loss of the surface area and the sulfur content of the deactivated catalysts by SO_2 strongly suggest the deposition

of a sulfur species as a deactivating agent on the catalyst surface. CuHM catalyst exhibited a higher sulfur deposition on the catalyst surface than HM catalyst. It well agrees not only with the decreasing trend of their BET surface areas but with milder deactivation of HM catalyst than CuHM catalyst. It was also observed by Ham *et al.* (25) for the reduction of NO by NH_3 over CuHM catalyst. In addition, the copper content of the catalysts such as CuHM (3.5 wt%) and CuNZA (1.8 wt%) also plays a crucial role for the loss of surface area by SO_2 and the deposition of sulfur on the catalyst surface.

TGA and TPSR. TGA for the deteriorated catalysts by SO_2 was made to observe the decomposition of a deactivating agent formed on the catalyst surface. As shown in Fig. 2A, the continuous weight loss up to about 500°C was examined over the fresh HM catalyst, which is mainly due to the desorption of the adsorbed water on the catalyst surface. The weight loss pattern of HM catalyst after the reduction of NO by C_2H_4 without SO_2 was similar to that of the fresh catalyst. However, it differs from the pattern for the catalyst deactivated by SO_2, which exhibits the steep weight loss rate at the ramping temperature of about 470°C.

Although the weight loss trend of the catalyst without SO_2 was almost analogous to that of HM catalyst, the TGA trend of CuHM catalyst deactivated by SO_2 was distinctive as shown in Fig. 2B. It exhibited the significant weight change at the temperature ranges from 420 to 680°C. The degree of the weight loss of CuHM catalyst deactivated by SO_2 seems to be much more severe than that of the deactivated HM catalyst. It is probably due to the difference in the amount of sulfur deposits on the catalyst surface.

Although the fresh CuNZA catalyst shows the similar weight loss to HM and CuHM catalysts, the catalyst after reaction with SO_2 presented the unique TGA patterns, as revealed in Fig. 2C. The weight loss of CuNZA catalyst deactivated by SO_2 initiating at about 400°C was much more significant than that of the synthetic zeolites, even though the sulfur deposition of the natural zeolite is much less. It is mainly due to another compound formed on the catalyst surface during the course of reaction such as a reaction intermediate as shown in Fig. 2C. c for the catalyst after reaction without SO_2. It should be noted that the TGA simply exhibits the total weight loss of the catalyst, regardless of the composition of the compounds. It will be further examined by TPSR. The TGA pattern for the deactivated catalysts also suggests the presence of a deactivating agent on the catalyst surface causing the decrease of the $deNO_x$ performance during the course of NO removal reaction with SO_2.

The surface sulfur compound on the deteriorated catalysts by SO_2 was carefully examined by TPSR, which may provide the information on the major species on the catalyst surface responsible for the loss of NO removal activity by SO_2. As depicted in Fig. 3, the desorption of SO_2 from the

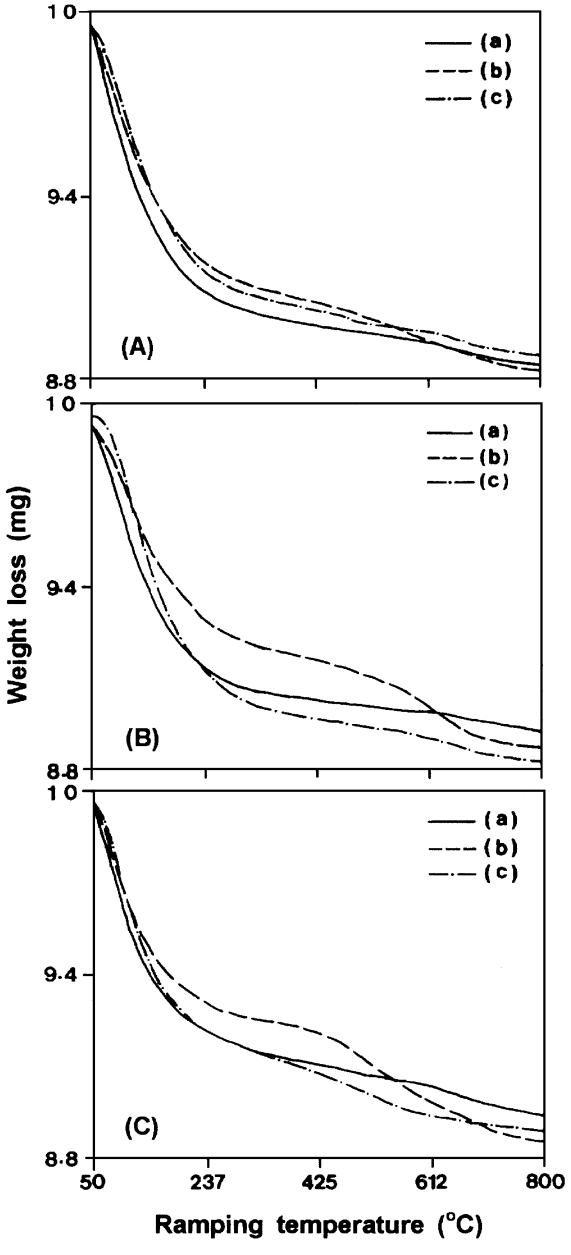

FIG. 2. TGA profile for the deactivated catalysts by SO_2: HM (A); CuHM (B); CuNZA (C). (a) fresh catalyst; (b) after reaction with SO_2; (c) after reaction without SO_2.

surface of the deactivated catalysts was evidently observed at temperatures higher than 400°C, regardless of the types of catalyst employed in the present study. The maximum desorption peak of SO_2 over HM catalyst was developed at 630°C. CuHM catalyst showed an unique desorption profile of SO_2 compared to that of HM catalyst, which exhibits three kinds of maximum desorption peaks at 450, 600, and 680°C. The desorption pattern of SO_2 for CuNZA catalyst is quite similar to that of CuHM catalyst. It may be due to the peculiar role of Cu^{2+} ion for the formation of a deactivating agent on the catalyst surface. In addition, the amount of

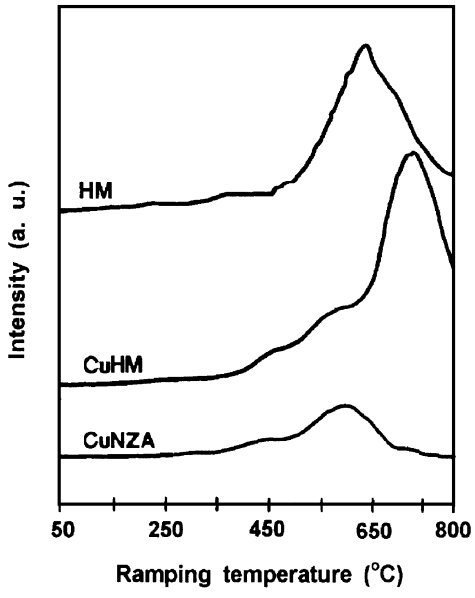

FIG. 3. TPSR profile for the deactivated catalysts by SO_2.

SO_2 desorption from the catalyst surface was proportional to the sulfur deposition of the catalyst as listed in Table 1, although the weight loss of CuNZA catalyst by TGA differs from the catalyst sulfur contents.

XPS and Raman. S 2p XPS spectra for the deactivated catalysts by SO_2 were examined to identify a sulfur compound as a deactivating agent on the catalyst surface. Figure 4 shows S 2p bands on the surface of the deteriorated catalysts. The S 2p line at the binding energy of 169.4 eV was observed for the synthetic zeolite catalysts, HM and CuHM, deactivated by SO_2. It is well known that XPS bands at 161.0 to 162.8 eV (26–28) and at about 164.0 eV (26, 28, 29) of the binding energies represent sulfide and elemental sulfur, respectively. The peaks at 167.8 to 171.0 eV, however, can be uniquely found for sulfates (26, 30). It indicates that the sulfur compound deposited on the surface of the deactivated catalysts exists in the form of sulfate (SO_4^{2-}) species which may be mainly attributed to the loss of the catalytic activity for NO removal reaction by SO_2.

The similar S 2p XPS line to CuNZA catalyst deactivated by SO_2 was also observed, as depicted in Fig. 4. The peak at 168.4 eV of the binding energy appeared over the catalyst, indicating that the sulfur compound on the catalyst surface also exists in the form of sulfate species. It should be noted that the sulfate species on CuNZA catalyst exhibited XPS band at lower binding energy than that on the synthetic zeolite catalysts.

The Raman shift for the deactivated catalysts by SO_2 was examined to further identify the sulfur species on the catalyst surface. The Raman spectra for the synthetic zeolite catalysts deactivated during the course of NO reduction by C_2H_4 in the presence of SO_2 are shown in Figs. 5A and B. The band shift at about 975 cm^{-1} was evident for HM and CuHM catalysts after the reaction with SO_2. When the fresh catalyst treated with a 0.2 *N* H_2SO_4 solution followed by drying at 300°C for 3 h was employed as a reference, it also exhibited the Raman shift similar to the deactivated catalysts by SO_2.

Figure 6 shows the Raman spectra for CuNZA catalyst deactivated by SO_2 included in the feed gas stream. The absorption band due to the sulfate on the catalyst surface was also found in the similar region, 973 cm^{-1} to that of HM and CuHM catalysts shown in Fig. 5. The prominent absorption band at 1120 cm^{-1} was notably observed, regardless of the catalysts employed in the present work. It is probably due to silicates contained in the zeolite catalysts as an impurity (31).

In addition, the Cu 2p XPS line of Cu-exchanged zeolite catalysts, CuHM and CuNZA, was also examined to investigate the effect of the sulfate species on the chemical surrounding of the copper ions on the catalyst surface, as

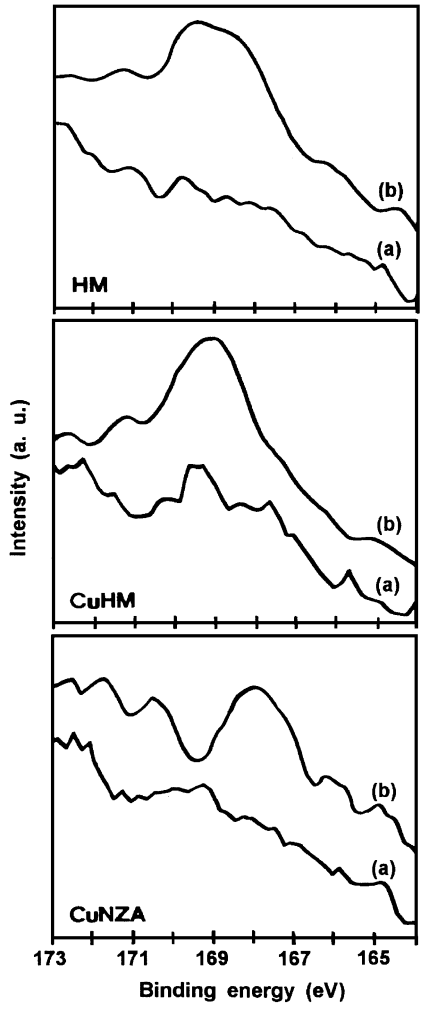

FIG. 4. S 2p XPS spectra for the deactivated catalysts by SO_2: (a) after reaction without SO_2; (b) after reaction with SO_2.

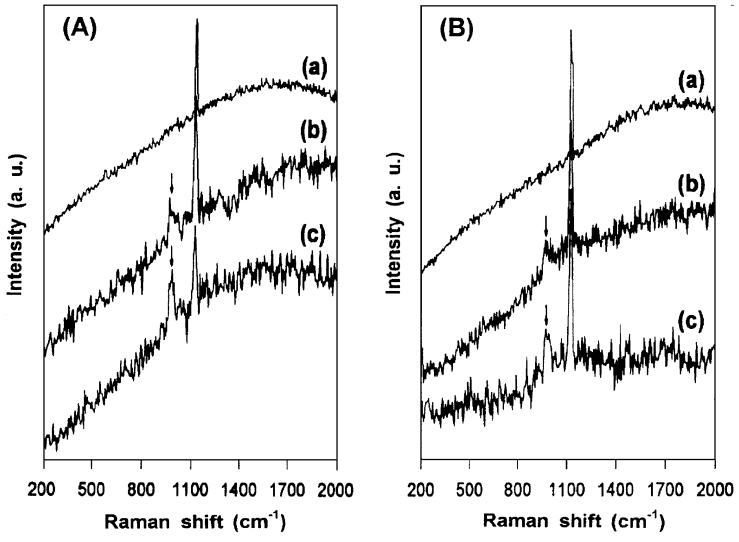

FIG. 5. Raman spectra for the synthetic mordenite catalysts deactivated by SO_2: HM (A) and CuHM (B). (a) fresh catalyst; (b) after reaction with SO_2; (c) fresh catalyst treated with a 0.2 *N* H_2SO_4 solution.

depicted in Fig. 7. Each of the $j = 1/2$ and 3/2 components over CuO and Cu_2O, respectively, as a reference for divalent and monovalent copper compounds exhibits a two-peak structure. It is in good agreement with the XPS spectra for the reference chemicals (32, 33). The main Cu 2p peaks as indicated by an upward arrow in Fig. 7 are found for both references: 932.2 to 933.7 eV (Cu 2p 3/2)and 952.3 to 954.0 eV (Cu 2p 1/2). However, the shake-up structures at about 942.2 (Cu 2p 3/2) and 962.5 eV (Cu 2p 1/2) are observed only for CuO, which is evidence for the existence of divalent copper. The copper-exchanged zeolite catalysts without and with SO_2 obviously appeared the Cu 2p 3/2 and 1/2 satellites at about 944.2 and 963.6 eV, respectively. It indicates that the chemical state of the copper ions on the

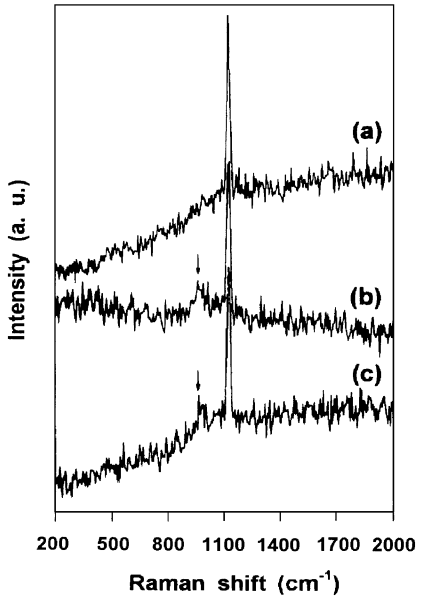

FIG. 6. Raman spectra for CuNZA catalyst deactivated by SO_2. (a) fresh catalyst; (b) after reaction with SO_2; (c) fresh catalyst treated with a 0.2 *N* H_2SO_4 solution.

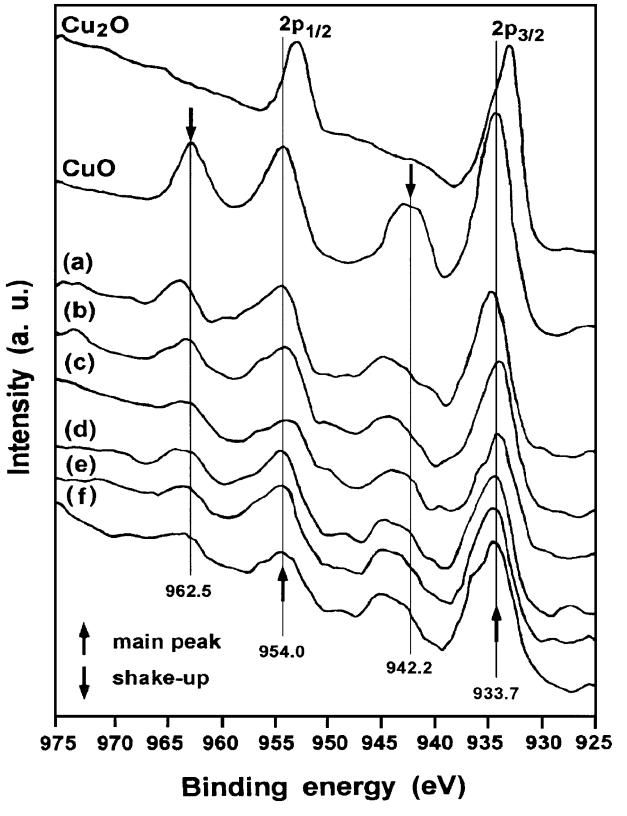

FIG. 7. Cu 2p XPS spectra for the deactivated catalysts by SO_2: CuHM (a, b, c) and CuNZA (d, e, f). (a, d) fresh catalyst; (b, e) after reaction without SO_2; (c, f) after reaction with SO_2.

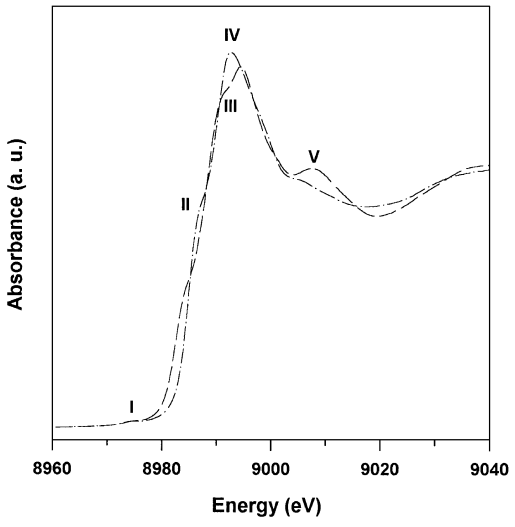

FIG. 8. Cu K-edge XANES spectra for $Cu(OH)_2$ (– – –) and $CuSO_4 \cdot 5H_2O$ (– · –) as a reference.

surface of the catalysts was not altered at all, even during the course of the reduction of NO by hydrocarbons with SO_2.

XANES. The effect of the sulfate species on the electronic structure of Cu ions was further examined by XAS for the deactivated catalysts, CuHM and CuNZA, along with the references. As shown in Fig. 8, the Cu K-edge absorption peak at 8974 eV due to the 1s-3d transition (peak I) is observed for the cupric sulfate pentahydrate ($CuSO_4 \cdot 5H_2O$) and copper hydroxide ($Cu(OH)_2$) as a reference employed in this study which exhibit the typical characteristic of Cu K-edge structure of divalent copper (34). With peak II at about 8985 (1s-4p π transition, out-of-plane) and 8988 eV (1s-4p π transition, in-plane), the peak IV which reflects the 1s-4p σ (in-plane) transition also appeared for the reference chemicals (35, 36). Particularly, the peak V by multiple scattering was also observed for the references.

Figure 9A shows the Cu K-edge XANES spectra for CuHM catalyst after SCR reaction with and without SO_2. The pre-edge absorption peak I at 8974 eV was still maintained even after the reaction with SO_2. The edge position of the deactivated catalyst by SO_2 is also identical to that of the fresh catalyst, as well as that of the catalyst after reaction without SO_2. However, the slight alteration of absorption at 9000 to 9018 eV was found for the deactivated catalyst, compared to the catalyst after the reaction without SO_2.

Figure 9B presents the Cu K-edge absorption of CuNZA catalyst deactivated by SO_2. Peak I by the 1s-3d transition also appeared for the catalyst, indicating that the copper ions on the catalyst surface exist in divalent form even after reaction with SO_2. At the absorption region of the 1s-4p π transition (out-of-plane), the catalyst after reaction with and without SO_2 is notably distinctive to the fresh catalyst. However, the new absorption peak at the position was observed for the catalyst, regardless of the presence of SO_2 in the feed gas stream. It is not primarily due to the effect of SO_2 on the catalyst for the reduction of NO by C_3H_6.

DISCUSSION

Cause of the Deactivation of Mordenite-Type Zeolite Catalysts by SO_2

The effect of SO_2 on NO removal activity of mordenite-type zeolite catalysts for the reduction of NO by hydrocarbons has been already examined in the previous study (23). The catalyst deactivation by SO_2 significantly depended not only on the types of catalyst but on the cations included in the zeolites (23). In the present work, the characterizing methods such as TGA, TPSR, XPS, Raman, and XAS, along with the measurements of the surface area and sulfur content of the deactivated catalysts were employed to elucidate the cause of the loss of NO reducing activity by SO_2.

The HM catalyst exhibited lower sulfur content on the catalyst surface than that of the CuHM catalyst. As listed in Table 1, HM and CuHM catalysts after SCR reaction with

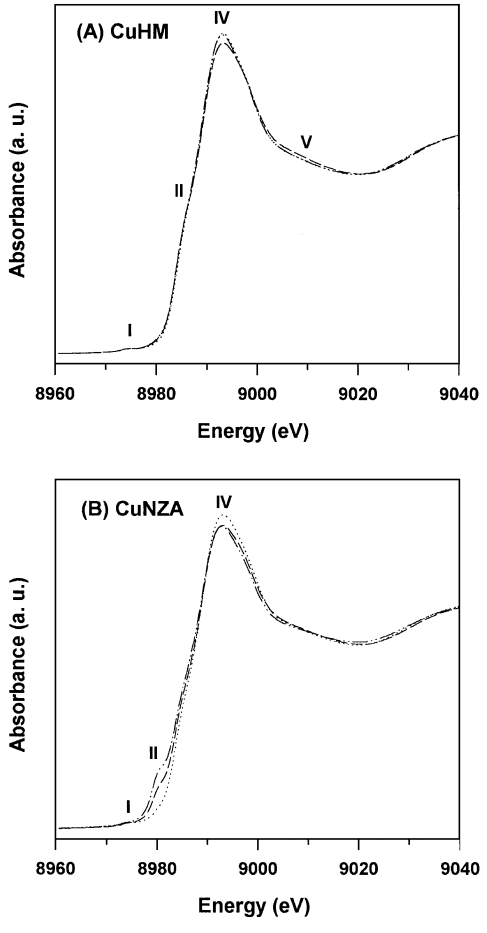

FIG. 9. Cu K-edge XANES spectra for CuHM (A) and CuNZA (B) catalysts deactivated by SO_2: (· · ·) fresh catalyst; (- · -) after reaction without SO_2; (- - -) after reaction with SO_2.

SO_2 contain the sulfur depositions of 1.10 (0.34 mmol SO_4^{2-}/g-cat) and 1.86 wt% (0.58 mmol SO_4^{2-}/g-cat), respectively. It shows that 1 mol of Cu^{2+} ion in the CuHM catalyst was occupied by about 1.04 mol of SO_4^{2-}, while 1 mol of H^+ in the HM catalyst by 0.15 mol of SO_4^{2-}. It also reveals that the population of SO_4^{2-} on Cu^{2+} ions in the CuHM catalyst is about seven times higher than that of the HM catalyst. It well agrees with the previous observation that the HM catalyst has shown stronger sulfur tolerance than the CuHM catalyst (23). It indicates that the formation of a deactivating agent containing a sulfur species on the catalyst surface was notably promoted by Cu ions in the zeolite catalyst. Therefore, the sulfur compound is dominantly responsible for the loss of the $deNO_x$ performance of the catalysts during the course of a SCR reaction in the presence of SO_2. The decrease of NO removal activity of the HM catalyst in two steps is probably due to the pore blockage by the deactivating agent through the initial transition period of the catalyst deactivation by SO_2. However, the sudden loss of $deNO_x$ activity was not observed for copper-containing catalyst, except in the early stage of the reaction, since the deactivating agent can be formed faster on CuHM than on HM catalyst. It should be noted that the oxidation capability of the catalyst, SO_2 to SO_3 is much higher for copper-containing catalyst than for copper free catalyst (25).

The sulfur deposition on CuNZA catalyst and the loss of its surface area after reaction with SO_2 were milder than those of CuHM catalyst. The molar ratio of SO_4^{2-}/Cu^{2+} of CuNZA catalyst is approximately 0.57 (0.17 mmol SO_4^{2-}/g-cat). It shows that the occupation of SO_4^{2-} per Cu^{2+} ion on the catalyst surface is about 60% of the SO_4^{2-}/Cu^{2+} ratio of CuHM catalyst. However, the reaction rate of the CuNZA catalyst for NO reduction has immediately decreased from 10.0×10^{-5} to 3.2×10^{-5} mmol/g · s, when 1000 ppm of SO_2 were admitted to the feed gas stream. It reveals that the catalyst is very sensitive to the deactivation by SO_2, even though it exhibited a better maintenance of NO removal activity than the synthetic mordenite catalysts with H_2O vapor in the feed gas stream without SO_2 (16). The catalyst deactivation by the carbonaceous compounds deposited on the surface of CuNZA catalyst had not been anticipated during the course of reaction without SO_2 as observed in Fig. 1. Therefore, the loss of the $deNO_x$ activity of CuNZA catalyst in the presence of SO_2 is primarily due to the formation of the sulfur species on the catalyst surface.

In addition, the surface area of the fresh CuHM catalyst is about two times that of the fresh CuNZA catalyst. The amounts of SO_4^{2-} deposition, based upon the surface area of HM, CuHM, and CuNZA catalysts are 0.76, 1.34, and 0.82 μmol/m^2, respectively. The amounts of SO_4^{2-} deposited on the synthetic mordenites are proportional to the extent of the catalytic activity loss by SO_2. Although the CuNZA catalyst maintains lower surface coverage of SO_4^{2-} than the CuHM catalyst, the former showed a much more severe decrease of the $deNO_x$ activity than the latter, as shown in Fig. 1. It may be due to the structural deficiency of the natural zeolite by impurities contained in the ores of natural zeolite. It should be noted that the NZA catalyst mainly includes mordenite-type zeolite but still contains impurities such as feldspar and various kinds of metal oxide. They may be useful for water tolerance of the present catalytic reaction system, but not for sulfur tolerance. The structure and impurities of the CuNZA catalyst has been extensively examined in the previous work (24).

After the SCR reaction with SO_2, the degree of decrease in the surface area of the CuHM catalyst was more severe than that of the HM catalyst. The surface area of the CuNZA catalyst after the reaction with SO_2 also decreased to 139 m^2/g. The loss of the catalyst surface area probably arises from an unique pore structure of mordenite-type zeolites employed in the present study. Mordenite contains a two-dimensional channel network which comprises near-cylindrical noninterconnecting main channels (6.95×5.81 Å) running in the crystallographic (001) direction and small side pockets (3.87×4.72 Å) (37). The kinetic diameter (σ) of the largest molecules being able to diffuse into the main channels of mordenite is about 6.20 Å.

Since the bond distance between S and O atoms in SO_4^{2-} is known to be 1.49 Å (38), the diagonal length of O-S-O bond in the SO_4^{2-} anion is approximately 2.58 Å. Note that it was calculated from a tetrahedral structure of SO_4^{2-}. When two SO_4^{2-} anions are adsorbed on the cations (H^+ and/or Cu^{2+}) on opposite sides of the identical channel of mordenite, its effective pore diameter can be easily reduced to about 1.84 Å which is too small even for N_2 ($\sigma = 3.64$ Å) to diffuse into the partially blocked main pores. It indicates that the surface area of the mordenite-type zeolite catalysts employed in the present study can be significantly decreased by deposition of SO_4^{2-} on the catalyst surface. The recent results by Ham *et al.* (24) strongly support such a speculation for the loss of the surface area of the catalysts after reaction with SO_2. They have observed that HM, CuHM31 (2.3 wt% Cu), and CuHM58 (4.2 wt% Cu) catalysts lose their fresh surface areas by 35, 50, and 100%, respectively, even though NH_3 is adsorbed on the catalyst surface at room temperature.

The TGA pattern of the deactivated catalysts by SO_2 quite differed from those of the catalysts after the SCR reaction without SO_2, regardless of the types of catalyst employed in the present work. It is due to the deposition of the sulfur species on the catalyst surface after the reduction of NO by hydrocarbons with SO_2. Although the weight loss of the deactivated catalysts by the decomposition of the sulfur compound as a deactivating agent is mainly initiated at temperatures higher than about 400°C, the trend of the weight loss of the CuHM catalyst was very distinctive compared to that of the HM catalyst, but not to the CuNZA catalyst, as observed in Fig. 2. The copper ion-exchanged

catalysts have also exhibited the poor activity maintenance for NO removal reaction with SO_2, as revealed in Fig. 1. It indicates that the copper ions in the zeolite catalysts are strongly involved to the mechanism of the catalyst deactivation by SO_2.

The sulfur compound as a deactivating agent examined by TGA was explicitly observed during the TPSR for the catalysts deactivated by SO_2. Its desorption profile from the catalyst surface varied with respect to the existence of cations on the surface of the zeolite catalysts employed in this work. The maximum desorption peak of SO_2 for the HM catalyst appeared at about 630°C along with the initial desorption at 470°C. Based upon the comparison between the TGA and TPSR spectra of the catalyst with and without SO_2, the apparent loss of the catalyst weight at temperatures higher than about 470°C is mainly due to the thermal decomposition of the sulfur species deposited on the catalyst surface.

The desorption profile of SO_2 for CuHM and CuNZA catalysts quite differed from that of the HM catalyst, which exhibited three kinds of desorption peak, as shown in Fig. 3. Compared to the TPSR pattern of the HM catalyst deactivated by SO_2, the copper ions accelerate the formation of the sulfur species on the catalyst surface. Its major decomposition into SO_2 on the CuHM catalyst was also observed at a higher desorption temperature than on the HM catalyst, indicating that the sulfur compound strongly interacts with Cu ions on the catalyst surface. The desorption pattern of SO_2 for the CuNZA catalyst is basically similar to that of the CuHM catalyst. The TPSR spectra for the deactivated catalysts can readily identify the presence of the deactivating agent formed on the catalyst surface. The amount of SO_2 desorption from the catalyst surface at temperatures above 400°C is proportional to the sulfur content of the HM and CuHM catalysts, as well as with the trend of their weight loss observed in Fig. 2 by TGA. However, the degree of SO_2 desorption at the temperatures differs from that of the weight loss of CuNZA catalyst by TGA. It is presumably due to the additional loss by the other compounds, including the reaction intermediates on the catalyst surface, as extensively discussed before. The desorption of other compounds such as CO_2, CO, H_2O, and CH_4 was also observed for the catalysts employed for TPSR study. Note that the amount of SO_3 desorbed from all catalysts was relatively negligible.

Based upon the alteration of BET surface area and sulfur content of the deactivated catalysts by SO_2, as well as the patterns of TGA and TPSR of the catalysts, the formation of the sulfur species as a deactivating agent on the catalyst surface could be identified, regardless of the types of catalyst and reductant employed in the present work. It is strongly bounded on the surface of the catalysts, as it was mainly decomposed into SO_2 at temperatures above 500°C.

The XPS and Raman studies of the deactivated catalysts also provided a chemical nature of the sulfur species as a deactivating agent examined by the TGA and TPSR. The S 2p XPS line of the deactivated catalysts was typically observed as the binding energies ranged from 168.4 to 169.4 eV, as shown in Fig. 4. With the XPS results for S 2p binding energy of sulfur compounds such as elemental sulfur, sulfide, and sulfate (26–30), the sulfur compound on the surface of the deactivated catalysts by SO_2 exists in the form of a sulfate species. It might be further confirmed by the Raman spectra of the deactivated and H_2SO_4-treated catalysts revealing the peak at about 975 cm^{-1} due to the formation of the sulfate on the catalyst surface. It plays a crucial role for the apparent loss of the deNO_x activity of the zeolite catalysts during the course of the reduction of NO by hydrocarbons with SO_2. The S 2p binding energy of the CuNZA catalyst was slightly altered, compared to that of the HM and CuHM catalysts, about 1.0 eV. It may indicate that the sulfate species on CuNZA catalyst is less solid-like than that on the synthetic zeolite catalysts (39). It agrees well with the TPSR spectra, where the sulfur compound on the surface of HM and CuHM catalysts was decomposed at higher temperatures than that on the CuNZA catalyst.

A Role of Cu^{2+} Ions for the Catalyst Deactivation by SO_2

The effect of SO_2 on the selective reduction of NO by hydrocarbons over transition metal-exchanged zeolite catalysts has been examined (9, 15, 20–23), but the deactivation mechanism by SO_2 is not clear yet. There is an agreement in the literature that the deNO_x efficiency is significantly reduced by exposing the catalysts to the feed gas stream containing SO_2. The decreasing rate of the activity for NO reduction by hydrocarbons in the presence of SO_2 has been faster over the Cu-exchanged mordenite-type zeolite catalysts than over the catalyst without Cu ions. It has been also observed for the reduction of NO by NH_3 with SO_2 (25). It implies that the copper ions exchanged in the zeolite catalysts play an important role for the catalyst deactivation by SO_2.

Based upon the characteristics of the deactivated HM and CuHM catalysts by SO_2, the degree of the decrease of surface area and the increase of sulfur deposition for the CuHM catalyst is more significant than for the HM catalyst. In addition, the TGA and TPSR profiles of the CuHM catalyst quite differed from those of the copper-free catalyst. These observations for the catalyst deactivation by SO_2 may be evidence for the unique role of Cu ions which not only enhance the formation of the sulfate species as a deactivating agent but also stabilize the agent on the catalyst surface. Since the NZA catalyst apparently showed low NO reducing efficiency within the ranges of the reaction temperatures covered in this study, less than 20% of NO conversion even without SO_2, the effect of SO_2 on the reducing activity of the catalyst has not been examined. The copper-free natural zeolite catalyst, NZA, is believed to be much less

sensitive to SO_2 than the CuNZA catalyst, as observed for the synthetic zeolite catalysts, HM and CuHM. Therefore, the role of the copper ions in the natural zeolite catalyst for the deactivation by SO_2 may be similarly anticipated, as it was for the synthetic zeolite catalyst.

The inner-shell XPS spectra of divalent copper compounds show strong shake-up to the main peak, which structure is very sensitive to the chemical surrounding the copper (40). Therefore, the energy separation (ΔE_{ms}) between their satellite and main peak is very unique. As shown in Fig. 7, ΔE_{ms} for CuO is approximately 8.5 eV. The value of ΔE_{ms} for CuHM and CuNZA catalysts, 9.5 eV, was consistently maintained even for the catalysts deactivated by SO_2. This indicates that the electronic environment of the copper ions on the catalyst surface may not be significantly altered, even after the reduction of NO under the deactivating condition including SO_2. However, the copper sulfate pentahydrate ($CuSO_4 \cdot 5H_2O$) as a reference exhibited the main-satellite separation of 7.5 eV. It also reveals that the sulfate species on the surface of the deactivated catalysts does not exist in the form of $CuSO_4 \cdot 5H_2O$.

Fundamentally, ΔE_{ms} of Cu(II) compounds becomes smaller as the electro-negativity of the ligand increases, i.e., 6.2 eV for CuF_2 (41), 8.5 eV for CuO (32), 8.6 eV for $CuCl_2$ (41), and 9.5 eV for $CuBr_2$ (41). The Pauling-scale electronegativities of F, O, Cl, and Br as a ligand are 3.98, 3.44, 3.16, and 2.96, respectively (42). The group electro-negativity of SO_4 is also 3.7, as previously calculated by McDaniel and Yingst (43). Therefore, ΔE_{ms} for $CuSO_4$, 7.5 eV lies between CuF_2 and CuO. The sulfate compound identified by XPS and Raman observations for the deactivated catalysts may exhibit similar electro-negativity to SO_4. However, not only ΔE_{ms} of the copper-ion-exchanged catalysts, 9.5 eV is much higher than that of $CuSO_4$, but also the energy separation is not distinctive, even for the catalysts deactivated by SO_2. It may reveal that the sulfate species formed on the catalyst surface does not notably alter the chemical environment of the copper ions in the zeolite catalysts.

The XANES spectra of CuHM and CuNZA catalysts can also draw the information for the electronic structure of the copper ions on the catalyst surface. The 1s-3d transition was observed for cupric sulfate pentahydrate and copper hydroxide, as well as for the catalyst deactivated by SO_2, but the significant 1s-4p π (in- and out-of-planes) transition and multiple scattering (35, 36) did only for the references. Based upon the Cu K-edge XANES spectra for the catalysts depicted in Figs. 8 and 9, no electronic environment of the copper ions contained in the zeolite catalysts was analogous to that of the references. It reveals that the sulfate species formed during the course of the NO removal reaction with SO_2 was not similar to the cupric sulfate pentahydrate which contains the copper ion surrounded by a tetragonally distorted octahedron of oxygen atoms (44). It might partially surround the copper ions on the catalyst surface, as previously suggested by Choi *et al.* (45) and Hamada *et al.* (46).

Since Cu ions on the zeolite surface exist in an isolated environment, they may interact with the sulfate species on the catalysts deactivated by SO_2. They may also contain the characteristic of the coordinate covalent bond, where Cu ions and sulfate species may act as a Lewis acid and base, respectively (47). The ligands such as H_2O, NH_3, $(C_2H_5)_3P$, and CO as a molecule and Cl^-, CN^-, OH^-, NO_2^-, and $C_2O_4^{2-}$ as an ionic species should at least contain a lone pair of electrons to form a coordinate covalent bond between metal ions and ligands (48). It should be noted that the sulfate species formed on the deactivated catalysts contains the lone pairs of electrons on O atoms which surround the S atom of an SO_4 group. It suggests that the sulfate species can interact with Cu ions on the surface of the zeolite catalysts.

CONCLUSIONS

The CuHM catalyst exhibited higher sulfur deposition on the catalyst surface than the HM catalyst, which agrees well with the loss of their BET surface area. It also supports that the HM catalyst showed milder deactivation of NO removal activity than the CuHM catalyst. CuNZA, a strong water-tolerant deNO_x catalyst, also shows deactivation by SO_2. The sulfur deposition and the reduction of the surface area of the catalyst are apparent as the deactivation proceeds. TGA and TPSR for the deactivated catalysts by SO_2 suggest the formation of a deactivating agent containing sulfur on the catalyst surface.

The sulfur species as a deactivating agent is strongly bounded on the surface of the catalysts, as it is mainly decomposed into SO_2 at temperatures higher than 500°C. It exists in the form of sulfate (SO_4^{2-}) which mainly causes the loss of the deNO_x activity of the catalysts as examined by XPS and Raman. Based upon the XANES spectra for the CuHM and CuNZA catalysts after the reaction with SO_2, the sulfate species on the deactivated catalysts does not exist in the form of $CuSO_4 \cdot 5H_2O$. It simply interacts with Cu ions on the catalyst surface.

REFERENCES

1. Iwamoto, M., and Mizuno, N., *J. Auto. Eng.* **207**, 23 (1993) and therein references.
2. Held, W., Konig, A., Richter, T., and Puppe, L., *SAE Paper 900496* (1990).
3. Truex, T. J., Searles, R. A., and Sun, D. C., *Platinum Met. Rev.* **36**, 2 (1992).
4. Li, Y., and Armor, J. N., *Appl. Catal. B* **2**, 239 (1993). [*Appl. Catal. B* **3**, L1 (1993); *J. Catal.* **145**, 1 (1994); *Appl. Catal. B* **1**, L31 (1992)]
5. Yogo, K., Umeno, M., Watanabe, H., and Kikuchi, E., *Catal. Lett.* **19**, 131 (1993).
6. Demicheli, M. C., Hoang, L. C., Menezo, J. C., and Barbier, J., *Appl. Catal. A* **97**, L11 (1993).
7. Tabata, T., Kokitsu, M., and Okada, O., *Catal. Lett.* **25**, 393 (1994).

8. Zhang, X., Walters, A. B., and Vannice, M. A., *J. Catal.* **146**, 568 (1994).
9. Kim, M. H., Nam, I.-S., and Kim, Y. G., *Appl. Catal. B* **6**, 297 (1995).
10. Loughran, C. J., and Resasco, D. E., *Appl. Catal. B* **5**, 351 (1995).
11. Li, Y., Battavio, P. J., and Armor, J. N., *J. Catal.* **142**, 561 (1993).
12. Gopalakrishnan, R., Stafford, P. R., Davidson, J. E., Hecker, W. C., and Bartholomew, C. H., *Appl. Catal. B* **2**, 165 (1993).
13. Bethke, K. A., Alt, D., and Kung, M. C., *Catal. Lett.* **25**, 37 (1994).
14. Kharas, K. C. C., Robota, H. J., and Liu, D. J., *Appl. Catal. B* **2**, 225 (1993).
15. Tabata, T., Kokitsu, M., Okada, O., Nakayama, T., Yasumatsu, T., and Sakane, H., *Stud. Surf. Sci. Catal.* **88**, 409 (1994).
16. Kim, M. H., Nam, I.-S., and Kim, Y. G., *Stud. Surf. Sci. Catal.* **105**, 1493 (1997). [*Appl. Catal. B* **12**, 125 (1997)]
17. Grinsted, R. A., Zhen, H. W., Montreuil, C., Rokosz, M. J., and Shelef, M., *Zeolites* **13**, 602 (1993).
18. Yan, J. Y., Lei, G.-D., Sachtler, W. M. H., and Kung, H. H., *J. Catal.* **161**, 43 (1996).
19. Summers, T. C., and Baron, K., *J. Catal.* **57**, 380 (1979).
20. Iwamoto, M., Yahiro, H., Shundo, S., Yu-u, Y., and Mizuno, N., *Appl. Catal.* **69**, L15 (1991).
21. Mabilon, G., and Durand, D., *Catal. Today* **17**, 285 (1993).
22. Li, Y., and Armor, J. N., *Appl. Catal. B* **5**, L257 (1995).
23. Kim, M. H., Nam, I.-S., and Kim, Y. G., *in* "Proceedings of the 1st World Congress, Environmental Catalysis—For a better World and Life, Pisa, 1995" (G. Centi, S. Perathoner, C. Cristiani, and P. Forzatti, Eds.), p. 251. Societa' Chimica Italiana, Rome, 1995.
24. Kim, M. H., Hwang, U.-C., Nam, I.-S., and Kim, Y. G., *Catal. Today*, in press.
25. Ham, S.-W., Choi, H., Nam, I.-S., and Kim, Y. G., *Ind. Eng. Chem. Res.* **34**, 1616 (1995).
26. Chastain, J. (Ed.), "Handbook of X-ray Photoelectron Spectroscopy: A Reference Book of Standard Spectra for Identification and Interpretation of XPS Data," Perkin-Elmer, Minnesota, 1992.
27. Nefedov, V. I., Salyn, Y. V., Solozhenkin, P. M., and Pulatov, G. Y., *Surf. Interf. Anal.* **2**, 170 (1980).
28. Ebitani, K., Konno, H., Tanaka, T., and Hattori, H., *J. Catal.* **135**, 60 (1992).
29. Wang, T., Vazquez, A., Kato, A., and Schmidt, L. D., *J. Catal.* **78**, 306 (1982).
30. Xue, E., Seshan, K., van Ommen, J. G., and Ross, J. R. H., *Appl. Catal. B* **2**, 183 (1993).
31. Griffith, W. P., *J. Chem. Soc. A*, 1372 (1969).
32. Scrocco, M., *Chem. Phys. Lett.* **63**, 52 (1979).
33. Jernigan, G. G., and Somorjai, G. A., *J. Catal.* **147**, 567 (1994).
34. Bair, R. A., and Goddard III, W. A., *Phys. Rev. B* **22**, 2767 (1980).
35. Kosugi, N., Yokoyama, T., Asakura, K., and Kuroda, H., *Chem. Phys.* **91**, 249 (1984).
36. Smith, T. A., Penner-Hahn, J. E., Berding, M. A., Doniach, S., and Hodgson, K. O., *J. Am. Chem. Soc.* **107**, 5945 (1985).
37. Eberly, P. E., Jr., *J. Phys. Chem.* **67**, 2404 (1963).
38. Bianconi, A., *in* "X-ray Absorption: Principles, Applications, Techniques of EXAFS, SEXAFS, and XANES" (D. C. Koningsberger and R. Prins, Eds.), Vol. 92, p. 573. Wiley, New York, 1988.
39. Wagner, C. D., and Taylor, J. A., *J. Electron Spectrosc. Relat. Phenom.* **28**, 211 (1982).
40. Frost, D. C., Ishitani, A., and McDowell, C. A., *Mol. Phys.* **24**, 861 (1972).
41. van der Laan, G., Westra, C., Haas, C., and Sawatzky, G. A., *Phys. Rev. B* **23**, 4369 (1981).
42. Allred, A. L., *J. Inorg. Nucl. Chem.* **17**, 215 (1961).
43. McDaniel, D. H., and Yingst, A., *J. Am. Chem. Soc.* **86**, 1334 (1964).
44. Bacon, G. E., and Curry, N. A., *Proc. Roy. Soc. A* **266**, 95 (1962).
45. Choi, E. Y., Nam, I.-S., Kim, Y. G., Chung, J. S., Lee, J. S., and Nomura, M., *J. Mol. Catal.* **69**, 247 (1991).
46. Hamada, H., Matsubayashi, N., Shimada, H., Kintaichi, Y., Ito, T., and Nishijima, A., *Catal. Lett.* **5**, 189 (1990).
47. Huheey, J. E., "Inorganic Chemistry: Principles of Structure and Reactivity," 3rd ed., p. 359. Harper & Row, New York, 1983.
48. Basolo, F., and Johnson, R. C., "Coordination Chemistry," 2nd ed., p. 17. Whitstable Litho, New York, 1986.